Progress In Electromagnetics Research, Vol. 140, 31–42, 2013

AN APPROACH FOR MULTI-BAND BANDPASS FILTER DESIGN BASED ON ASYMMETRIC HALF-WAVELENGTH RESONATORS

Xiuping Li[1, 2, *] and Huisheng Wang[1, 2]

[1]School of Electronic Engineering, Beijing University of Posts and Telecommunications, Beijing 100876, China

[2]Beijing Key Laboratory of Work Safety Intelligent Monitoring, Beijing University of Posts and Telecommunications, Beijing 100876, China

Abstract—This paper presents that the extra passband with two transmission zeros can be obtained by adding shunt open stubs to the asymmetric half-wavelength resonators structure. By using this method, a fourth or even higher passband with good selectivity and compact size can be obtained. Dual-band, tri-band and quad-band bandpass filters are demonstrated by using this method. The measured bandwidth is 80/180 MHz for the dual-band, 60/180/180 MHz for the tri-band and 130/360/170/70 MHz for the quad-band filter, respectively. The measured insertion loss for the dual-band, tri-band and quad-band filter is less than 2.7 dB, 2.5 dB and 2.9 dB at the center frequency. All the simulated results and the measured results agree well.

1. INTRODUCTION

Recent development in wireless communication and radar systems has presented new challenges to design and produce high-quality miniature components with multi-band performance. There are many methods to design multi-band filters, such as combining two single-band filters at different passband frequencies [1–5], adding defected stepped impedance resonator (DSIR) and microstrip stepped impedance resonator (MSIR) [6–9] or adding a couple of resonators [10–13]. The method of adding shunt open stub to the center of the resonator is used to design dual-band filter and there are three transmission zeros for the two passbands [14, 15]. The combination

Received 15 March 2013, Accepted 23 April 2013, Scheduled 22 May 2013

* Corresponding author: Xiuping Li (xpli@bupt.edu.cn).

of adding shunt open stub to the center of the resonator and adding resonators is used to design tri-band filter, where five transmission zeros for the three passbands [16–18].

This paper presents the applications of shunt open stubs for microstrip multi-band bandpass filter design. Theoretical analysis on obtaining multi-passband performance by adding shunt open stubs to the asymmetric half-wavelength resonators is introduced. By using this method, the fourth even higher passband can be obtained by adding shunt open stubs and the filter dimension is kept compact. Furthermore, in order to verify the method, the dual-band, tri-band and quad-band filters are fabricated and the expected responses are obtained. The simulated results and the measured results agree well.

The rest of the paper is organized as follows: the theoretical analysis with $ABCD$ matrix method is given to explain the new approach in Section 2. In Section 3, the dual-band, tri-band and quad-band filters are fabricated to verify the method. The conclusion is given in Section 4.

2. ANALYSIS OF THE ASYMMETRIC HALF-WAVELENGTH RESONATORS WITH SHUNT OPEN STUBS

In order to facilitate the analysis, the asymmetric half-wavelength resonators coupling structure with shunt open stub is design, as shown in Fig. 1. The total length of one resonator is $2l_3 + l_2 + l_1 = \lambda_0 = 2$, where λ_0 is the guided wavelength at fundamental resonance. The l_4 is the shunt open stub ,which is connected to the resonator directly. The coupling between the two open ends of the resonators is simply expressed by the gap capacitance C_S [19, 20].

Inspecting the Fig. 1, the whole circuit represents a shunt circuit,

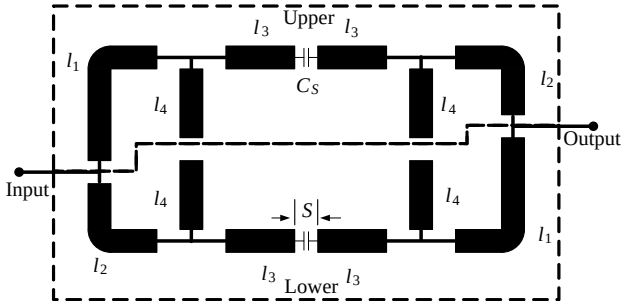

Figure 1. Configuration of asymmetric half-wavelength resonators coupling structure with shunt open stubs ($l_1 > l_2$).

as the dotted boxes shows, which consists of upper and lower sections. Each section is composed of l_1, l_2, l_3, l_4 and C_S. The $ABCD$ matrices for the upper and lower sections of the lossless shunt circuit are

$$\begin{bmatrix} A & B \\ C & D \end{bmatrix}_{upper} = M_1 M_4 M_3 M_C M_3 M_4 M_2 \tag{1a}$$

$$\begin{bmatrix} A & B \\ C & D \end{bmatrix}_{lower} = M_2 M_4 M_3 M_C M_3 M_4 M_1 \tag{1b}$$

with

$$M_n = \begin{bmatrix} \cos\beta l_n & jZ_0 \sin\beta l_n \\ jY_0 \sin\beta l_n & \cos\beta l_n \end{bmatrix} \quad (n = 1, 2, 3)$$

$$M_C = \begin{bmatrix} 1 & \frac{1}{j\omega C_S} \\ 0 & 1 \end{bmatrix} \quad M_4 = \begin{bmatrix} 1 & 0 \\ jY_0 \tan\beta l_4 & 1 \end{bmatrix}$$

where β is the propagation constant, Z_0 the characteristic impedance of the resonator, ω the angular frequency, and $Y_0 = 1/Z_0$. The Y-parameters for this circuit can be obtained by adding the upper and the lower section Y-parameters, which follow from (1a) and (1b), respectively. When the load is matching, S_{21} of the circuit can then be calculated from the total Y-parameters. The S_{21} for the whole circuit are

$$S_{21} = \frac{4Y_0 B}{Y_0^2 B^2 + Y_0 B\,(A_1 + A_2 + D_1 + D_2) + 4BC + D_1 A_2 + D_2 A_1 - D_1 A_1 - D_2 A_2} \tag{2}$$

with

$$\begin{aligned} A_1 = D_2 = {} & \cos\beta\,(l_1 + l_2 + 2l_3) - \cos\beta\,(l_2 + 2l_3)\sin\beta l_1 \tan\beta l_4 \\ & - \sin\beta\,(l_1 + 2l_3)\cos\beta l_2 \tan\beta l_4 + \sin\beta l_1 \cos\beta l_2 \sin 2\beta l_3 \tan\beta l_4^2 \\ & + \frac{Y_0}{\omega C_s}[\cos\beta\,(l_1 + l_3)\sin\beta\,(l_2 + l_3) \\ & - \sin\beta\,(l_2 + l_3)\sin\beta l_1 \cos\beta l_3 \tan\beta l_4 \\ & + \cos\beta\,(l_1 + l_3)\cos\beta l_2 \cos\beta l_3 \tan\beta l_4 \\ & - \sin\beta l_1 \cos\beta l_2 \cos\beta l_3^2 \tan\beta l_4^2] \\ D_1 = A_2 = {} & \cos\beta\,(l_1 + l_2 + 2l_3) - \cos\beta\,(l_1 + 2l_3)\sin\beta l_2 \tan\beta l_4 \\ & - \sin\beta\,(l_2 + 2l_3)\cos\beta l_1 \tan\beta l_4 + \cos\beta l_1 \sin\beta l_2 \sin 2\beta l_3 \tan\beta l_4^2 \\ & + \frac{Y_0}{\omega C_s}\,[\sin\beta\,(l_1 + l_3)\cos\beta\,(l_2 + l_3) \\ & - \sin\beta\,(l_1 + l_3)\sin\beta l_2 \cos\beta l_3 \tan\beta l_4 \\ & + \cos\beta\,(l_2 + l_3)\cos\beta l_1 \cos\beta l_3 \tan\beta l_4 \\ & - \cos\beta l_1 \sin\beta l_2 \cos\beta l_3^2 \tan\beta l_4^2] \end{aligned}$$

$$
\begin{aligned}
B_1{=}B_2 = {} & jZ_0\left[\sin\beta\left(l_1+l_2+2l_3\right)-\sin\beta\left(l_1+2l_3\right)\sin\beta l_2\tan\beta l_4\right.\\
& \left.-\sin\beta\left(l_2{+}2l_3\right)\sin\beta l_1\tan\beta l_4{+}\sin\beta l_1\sin\beta l_2\sin 2\beta l_3\tan\beta l_4^2\right]\\
& +\frac{1}{j\omega C_s}\left[\cos\beta\left(l_1+l_3\right)\cos\beta\left(l_2+l_3\right)\right.\\
& -\cos\beta\left(l_1+l_3\right)\sin\beta l_2\cos\beta l_3\tan\beta l_4\\
& -\cos\beta\left(l_2+l_3\right)\sin\beta l_1\cos\beta l_3\tan\beta l_4\\
& \left.+\sin\beta l_1\sin\beta l_2\cos\beta l_3^2\tan\beta l_4^2\right]\\
C_1{=}C_2 = {} & jY_0\left[\sin\beta\left(l_1+l_2+2l_3\right)+\cos\beta\left(l_1+2l_3\right)\cos\beta l_2\tan\beta l_4\right.\\
& \left.+\cos\beta\left(l_2{+}2l_3\right)\cos\beta l_1\tan\beta l_4{-}\cos\beta l_1\cos\beta l_2\sin 2\beta l_3\tan\beta l_4^2\right]\\
& +\frac{jY_0^2}{\omega C_s}\left[\sin\beta\left(l_1+l_3\right)\sin\beta\left(l_2+l_3\right)\right.\\
& +\sin\beta\left(l_1+l_3\right)\cos\beta l_2\cos\beta l_3\tan\beta l_4\\
& +\sin\beta\left(l_2+l_3\right)\cos\beta l_1\cos\beta l_3\tan\beta l_4\\
& \left.+\cos\beta l_1\cos\beta l_2\cos\beta l_3^2\tan\beta l_4^2\right]
\end{aligned}
$$

the transmission zeros can be found by letting $S_{21}{=}0$. For a small C_S, an approximate equation can be obtained as:

$$
\begin{aligned}
&\cos\beta(l_2{+}l_3)\cos\beta(l_1{+}l_3)-\cos\beta(l_2+l_3)\sin\beta l_1\cos\beta l_3\tan\beta l_4\\
&-\cos\beta(l_1{+}l_3)\sin\beta l_2\cos\beta l_3\tan\beta l_4{+}\sin\beta l_1\sin\beta l_2\cos\beta l_3^2\tan\beta l_4^2{=}0 \quad (3)
\end{aligned}
$$

further, Equation (3) can be expressed as:

$$
\begin{aligned}
&\left[\cos\beta(l_1+l_3)-\sin\beta l_1\cos\beta l_3\tan\beta l_4\right]\\
&\times\left[\cos\beta(l_2+l_3)-\sin\beta l_2\cos\beta l_3\tan\beta l_4\right]=0
\end{aligned}
$$

Generally, we assume $l_1 < \lambda_0/4$, $l_2 < \lambda_0/4$, $l_3 < \lambda_0/4$, $l_4 < \lambda_0/4$, where λ_0 is the guided wavelength at fundamental resonance. Thus, we can obtain $\sin\beta l_1\cos\beta l_3\tan\beta l_4 > 0$ and $\sin\beta l_2\cos\beta l_3\tan\beta l_4 > 0$. In addition, we assume $\sin\beta l_1\cos\beta l_3\tan\beta l_4 < 1$ and $\sin\beta l_2\cos\beta l_3\tan\beta l_4 < 1$. The two transmission zeros, f_1 and f_2 can be obtained as:

$$
f_1 = \frac{c\times n\times\arccos(\sin\beta l_1\cos\beta l_3\tan\beta l_4)}{2\pi\sqrt{\varepsilon_{eff}}(l_1+l_3)} \quad (4a)
$$

$$
f_2 = \frac{c\times n\times\arccos(\sin\beta l_2\cos\beta l_3\tan\beta l_4)}{2\pi\sqrt{\varepsilon_{eff}}(l_2+l_3)} \quad (4b)
$$

where ε_{eff} is the effective dielectric constant, n is the mode number, c is the speed of light in free space. After transformation, Equation (2) also can be expressed as:

$$
\begin{aligned}
&\left[\cos\beta(l_1+l_3+l_4)+\cos\beta l_1\sin\beta l_3\sin\beta l_4\right]\\
&\times\left[\cos\beta(l_2+l_3+l_4)+\cos\beta l_2\sin\beta l_3\sin\beta l_4\right]=0
\end{aligned}
$$

and thus the other two transmission zeros, f_3 and f_4, can be obtained as:

$$f_3 = \frac{c \times n \times \arccos(-\cos\beta l_2 \sin\beta l_3 \sin\beta l_4)}{2\pi\sqrt{\varepsilon_{eff}}(l_1 + l_3 + l_4)} \tag{5a}$$

$$f_4 = \frac{c \times n \times \arccos(-\cos\beta l_1 \sin\beta l_3 \sin\beta l_4)}{2\pi\sqrt{\varepsilon_{eff}}(l_2 + l_3 + l_4)} \tag{5b}$$

Equations (4) and (5) present the transmission zeros on the both sides of the first and second passband, respectively.

3. APPLICATIONS

Based on the above analysis, the dual-band, tri-band and quad-band passband filters are designed and fabricated. A commercial *TLX-0* dielectric substrate of *TACONIC* with the relative dielectric constant of 2.45 and thickness of 0.79 mm is chosen to fabricate the filters and Agilent's $N5071c$ network analyzer is used for measurement.

3.1. Dual-band Filter Design

The filter with shunt open stubs is designed and fabricated, as shown in Fig. 2. The asymmetric half-wavelength resonators filter without shunt open stubs is illustrated in Fig. 2(a). Figs. 2(b) and Fig. 2(c) show the filter with four and eight shunt open stubs.

As shown in Fig. 3, the center frequency of the filter is shifted from 2.4 GHz to 2.1 GHz. Meanwhile, the two transmission zeros on the

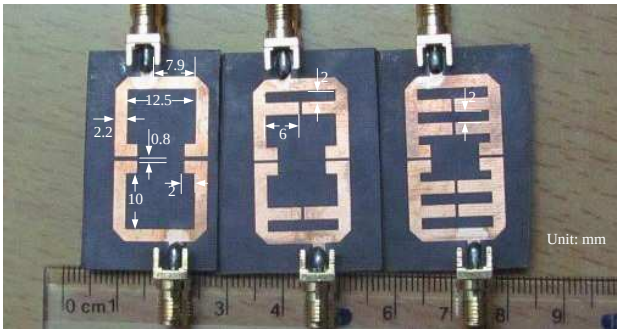

(a) (b) (c)

Figure 2. The photograph and size of the filters. (a) Filter without shunt open stubs. (b) Filter with four shun open stubs. (c) Filter with eight shunt open stubs.

both side of the first passband change from (2.16, 2.76) GHz to (1.92, 2.51) GHz by adding four shunt open stubs. It was also observed, after adding four shunt open stubs, an extra passband appeared at 6 GHz. Its corresponding transmission zeros on the both sides of the passband are (5.78, 6.18) GHz. The center frequency and bandwidth are 6 GHz and 270 MHz, respectively.

As shown in Fig. 3, the insertion loss of the passband is not good at 6 GHz and the return loss is worse than −10 dB. The reason is caused by the second harmonic of the fundamental passband, which locates too close to the new passband. To suppress the second harmonic of the fundamental passband, another four shunt short stubs are added [21, 22], as shown in Fig. 2(c). By using this method, the second harmonic can be weaken and shifted toward lower frequency.

As shown in Fig. 4, the center frequency of the first passband

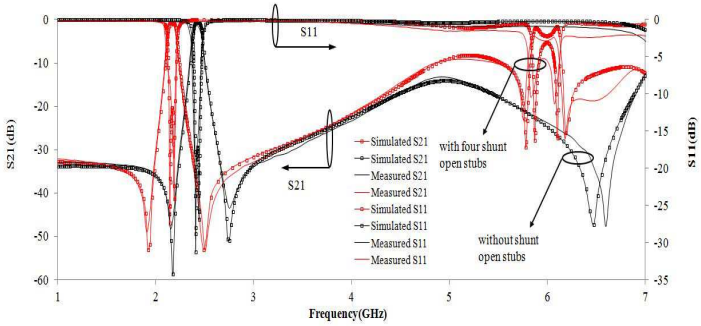

Figure 3. The responses of the filter without and with four shunt open stubs.

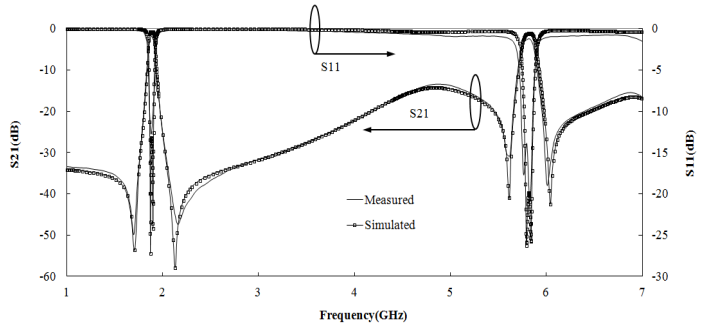

Figure 4. The responses of the filter with eight shunt open stubs.

is shifted toward lower frequency to 1.9 GHz and its bandwidth is 40 MHz. Meanwhile, the center frequency and bandwidth of the second passband are 5.8 GHz and 100 MHz, respectively. Moreover, in the passband, both the return loss and insertion loss are better than −10 dB and −2.7 dB, respectively.

3.2. Tri-band Filter Design

As above-mentioned, a passband with two transmission zeros can be obtained by shunt open stubs. We use this method to achieve the third passband by adding shunt open stubs. Fig. 5 shows the comparing of the tri-band filter with and without new shunt open stubs.

In Fig. 5, without new shunt open stubs, there are two passbands with the center frequency of 2.08 GHz and 6.04 GHz and there are the transmission zeros at 1.84 GHz, 2.39 GHz, 5.8 GHz and 6.32 GHz. New passband at 4.03 GHz is introduced by adding new shunt open stubs and the center frequencies of the two passbands are shifted to 1.57 GHz

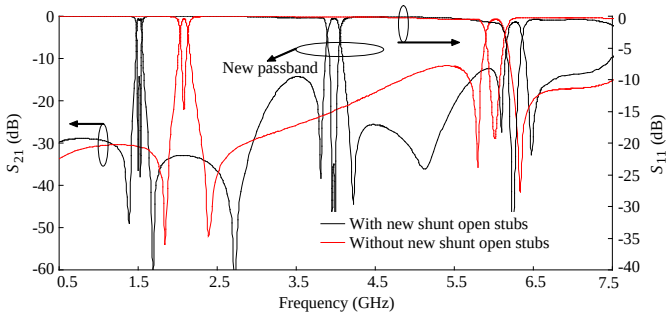

Figure 5. The comparison of the tri-band filter with and without new shunt open stubs.

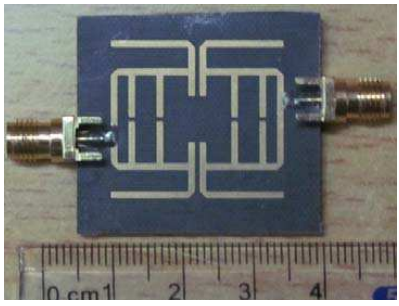

Figure 6. The photograph of tri-band filter.

and 6.29 GHz. The photograph of the tri-band filter is shown in Fig. 6. Obviously, comparing with the filter in Fig. 2(c), there are another four new shunt open stubs is added,which is folded for miniaturization. The responses of the tri-band filter are illustrated in Fig. 7. The measured −3 dB frequency ranges (fractional bandwidths) for the three passbands centered at 1.51, 4, and 6.26 GHz are 1.484–1.546 GHz (4.1%), 3.9–4.0 GHz (3.4%) and 6.19–6.34 GHz (2.3%), respectively. The minimum insertion losses measured for these three passbands are −2.5, −1.6, and −2.5 dB. The obtained transmission zeros from shunt open stubs are 1.385 and 1.685 GHz for the first passband, 3.810 and 4.224 GHz for the second band, and 6.104 and 6.481 GHz for the third band.

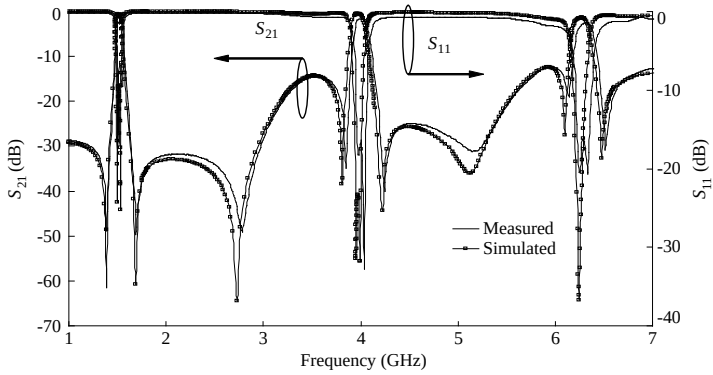

Figure 7. The responses of the tri-band filter.

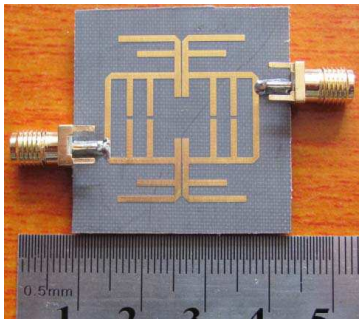

Figure 8. The photograph of quad-band filter.

3.3. Quad-band Filter Design

The photograph of the quad-band filter is illustrated in Fig. 8, and Fig. 9 shows the quad-band filter with and without new shunt open stubs. Without new shunt open stubs, there are three passbands with the center frequency of 1.51 GHz, 3.95 GHz and 6.47 GHz and there are transmission zeros at 1.26 GHz, 1.80 GHz, 3.69 GHz, 4.39 GHz, 6.09 GHz and 6.74 GHz. New passband at 7.13 GHz is introduced by adding new shunt open stubs and the center frequency of the three passbands are shifted to 1.37 GHz, 3.94 GHz and 6.09 GHz. The response of the quad-band filter is shown in Fig. 10. The measured −3 dB frequency ranges (fractional bandwidths) for the four passbands centered at 1.37, 3.9, 6.07 and 7.11 GHz are 1.29–1.42 GHz (9.5%), 3.72–4.08 GHz (9.2%), 5.96–6.13 GHz (2.8%) and 7.06–7.13 GHz (0.9%), respectively. The minimum insertion losses

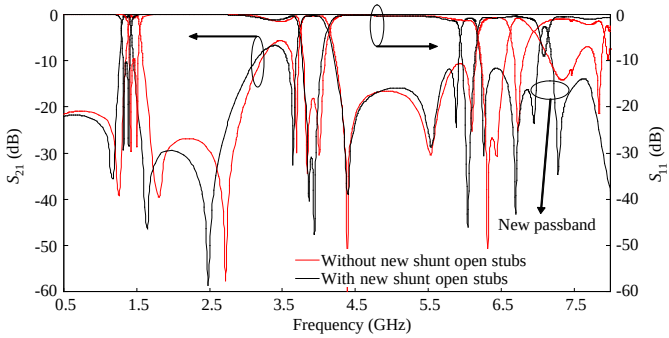

Figure 9. The comparison of the quad-band filter with and without new shunt open stubs.

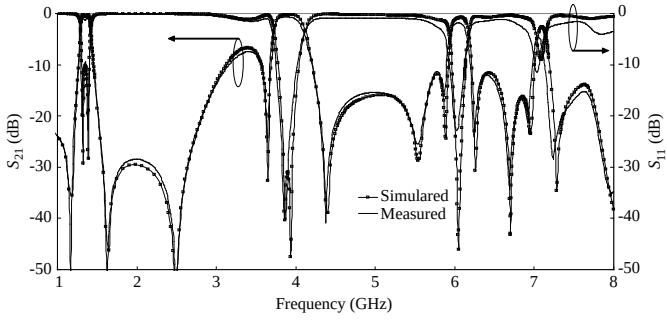

Figure 10. The responses of the quad-band filter.

measured for the four passbands are −1.2, −1.1, −2.3 and −2.9 dB. The transmission zeros from shunt open stubs are 1.17 and 1.63 GHz for the first passband, 3.65 and 4.37 GHz for the second band, 5.89 and 6.26 GHz for the third band and 6.95 and 7.28 GHz for the fourth band.

4. CONCLUSION

In this letter, a method to design multi-band filter is proposed and demonstrated, which is implemented by adding shunt open stubs to asymmetric half-wavelength resonators structure. The shunt open stubs can generate the second, third and forth passbands, while keeping the half-wavelength resonator as the first passband. The center frequencies of the passbands can be independently controlled by the length of the shunt open stubs and the half-wavelength resonator. To verify the method, the dual-band, tri-band and quad-band filters are fabricated and the expected responses are obtained. The simulated results and the measured results agree well.

ACKNOWLEDGMENT

This work was supported by National Natural Science Foundation of China (No. 61072009) and the support from Fundamental Research Funds for the Central Universities.

REFERENCES

1. Chen, C.-Y. and C.-Y. Hsu, "A simple and effective method for microstrip dual-band filters design," *IEEE Microw. Wireless Compon. Lett.*, Vol. 16, No. 5, 246–248, May 2006.
2. Chen, C.-Y. and C.-Y. Hsu, "A simple and effective method for microstrip dual-band filters design" *IEEE Microw. Wireless Compon. Lett.*, Vol. 16, No. 5, 246–248, May 2006.
3. Wu, G.-L., W. Mu, X.-W. Dai, and Y.-C. Jiao, "Design of novel dual-band bandpass filter with microstrip meander-loop resonator and CSRR DGS," *Progress In Electromagnetics Research*, Vol. 78, 17–24, 2008.
4. Zhao, L.-P., X.-W. Dai, Z.-X. Chen, and C.-H. Liang, "Novel design of dual-mode dual-band bandpass filter with triangular resonators," *Progress In Electromagnetics Research*, Vol. 77, 417–424, 2007.

5. Chen, C.-Y. and C.-C. Lin, "The design and fabrication of a highly compact microstrip dual-band bandpass filter," *Progress In Electromagnetics Research*, Vol. 112, 299–307, 2011.
6. Wu, B., C.-H. Liang, Q. Li, and P.-Y. Qin, "Novel dual-band filter incorporating defected SIR and microstrip SIR," *IEEE Microw. Wireless Compon. Lett.*, Vol. 18, No. 6, 392–394, June 2008.
7. Chiou, Y.-C. and J.-T. Kuo, "Planar multiband bandpass filter with multimode stepped-impedance resonators," *Progress In Electromagnetics Research*, Vol. 114, 129–144, 2011.
8. Chen, W.-Y., M.-H. Weng, S.-J. Chang, H. Kuan, and Y.-H. Su, "A new tri-band bandpass filter for GSM, WiMAX and ultra-wideband responses by using asymmetric stepped impedance resonators," *Progress In Electromagnetics Research*, Vol. 124, 365–381, 2012.
9. Ma, D., Z. Y. Xiao, L. Xiang, X. Wu, C. Huang, and X. Kou, "Compact dual-band bandpass filter using folded SIR with two stubs for WLAN," *Progress In Electromagnetics Research*, Vol. 117, 357–364, 2011.
10. Lee, S.-Y. and C.-M. Tsai, "New cross-coupled filter design using improved hairpin resonators," *IEEE Trans. Microwave Theory Tech.*, Vol. 48, No. 12, 2482–2490, February 2000.
11. Zhang, X. Y., C. H. Chan, Q. Xue, and B.-J. Hu, "Dual-band bandpass filter with controllable bandwidths using two coupling paths," *IEEE Microw. Wireless Compon. Lett.*, Vol. 20, No. 11, 616–618, June 2010.
12. Zhu, Y.-Z. and Y.-J. Xie, "Novel microstrip bandpass filters with transmission zeros," *Progress In Electromagnetics Research*, Vol. 77, 29–41, 2007.
13. Kuo, J.-T. and S.-W. Lai,"New dual-band bandpass filter with wide upper rejection band," *Progress In Electromagnetics Research*, Vol. 123, 371–384, 2012.
14. Doan, M. T., W. Che, K. Deng, and W. Feng, "Compact tri-band bandpass filter using stub-loaded resonator and quarter-wavelength resonator," *2011 China-Japan Joint Microwave Conference Proceedings (CJMW)*, 1–4,, April 2011.
15. Zhang, X. Y., J.-X. Chen, Q. Xue, and S.-M. Li, "Dual-band bandpass filters using stub-loaded resonators," *IEEE Microw. Wireless Compon. Lett.*, Vol. 17, No. 8, 583–585, June 2007.
16. Zhang, X. Y., Q. Xue, and B. J. Hu, "Planar tri-band bandpass filter with compact size," *IEEE Microw. Wireless Compon. Lett.*, Vol. 20, No. 5, 262–264, June 2010.

17. Chu, Q.-X., F.-C. Chen, Z.-H. Tu, and H. Wang, "A novel crossed resonator and its applications to bandpass filters," *IEEE Trans. Microwave Theory Tech.*, Vol. 57, No. 7, 1753–1759, July 2009.
18. Yang, C.-F., Y.-C. Chen, C.-Y. Kung, J.-J. Lin, and T.-P. Sun, "Design and fabrication of a compact quad-band bandpass filter using two different parallel positioned resonators," *Progress In Electromagnetics Research*, Vol. 115, 159–172, 2011.
19. Kwok, R. S. and J. F. Liang, "Characterization of high-Q resonators for microwave-filter applications," *IEEE Trans. Microwave Theory Tech.*, Vol. 47, No. 1, 111–114, January 1999.
20. Gupta, K. C., R. Garg, I. Bahl, and P. Bhartia, *Microstrip Lines and Slotlines,* 2nd Edition, Artech House, Boston, MA, 1996.
21. Zhang, J., J.-Z. Gu, B. Cui, and X.-W. Sun, "Compact and harmonic suppression open-loop resonator bandpass filter with tri-section SIR," *Progress In Electromagnetics Research*, Vol. 69, 93–100, 2007.
22. Wu, H.-W., S.-K. Liu, M.-H. Weng, and C.-H. Hung, "Compact microstrip bandpass filter with multispurious suppression," *Progress In Electromagnetics Research*, Vol. 107, 21–30, 2010.